

An individual-based model of ectotherm movement integrating metabolic and microclimatic constraints

Matthew Malishev^{1,2}  | C. Michael Bull³ | Michael R. Kearney² 

¹Centre of Excellence for Biosecurity Risk Analysis, Parkville, Australia

²School of BioSciences, University of Melbourne, Parkville, Australia

³School of Biological Sciences, Flinders University, Adelaide, Australia

Correspondence

Matthew Malishev

Email: matthew.malishev@gmail.com

Funding information

Australian Research Council, Grant/Award Number: DP0877384, DP110102813 and DP140101240

Handling Editor: Luca Börger

Abstract

1. An understanding of the direct links between animals and their environment can offer insights into the drivers and constraints to animal movement. Constraints on movement interact in complex ways with the physiology of the animal (metabolism) and physical environment (food and weather), but can be modelled using physical principles of energy and mass exchange. Here, we describe a general, spatially explicit individual-based movement model that couples a nutritional energy and mass budget model (dynamic energy budget theory) with a biophysical model of heat exchange. This provides a highly integrated method for constraining an ectothermic animal's movement in response to how food and microclimates vary in space and time.
2. The model uses R to drive a NetLogo individual-based model together with microclimate and energy- and mass-budget modelling functions from the R package "NICHEMAPR". It explicitly incorporates physiological and morphological traits, behavioural thermoregulation, movement strategies and movement costs. From this, the model generates activity budgets of foraging and shade-seeking, home range behaviour, spatial movement patterns and life history consequences under user-defined configurations of food and microclimates. To illustrate the model, we run simulations of the Australian sleepy lizard *Tiliqua rugosa* under different movement strategies (optimising or satisficing) in two contrasting habitats of varying food and shade (sparse and dense). We then compare the results with real, fine-scale movement data of a wild population throughout the breeding season.
3. Our results show that (1) the extremes of movement behaviour observed in sleepy lizards are consistent with feeding requirements (passive movement) and thermal constraints (active movement), (2) the model realistically captures majority of the distribution of observed home range size, (3) both satisficing and optimising movement strategies appear to exist in the wild population, but home range size more closely approximates an optimising strategy, and (4) satisficing was more energetically efficient than optimising movement, which returned no additional benefit in metabolic fitness outputs.
4. This framework for predicting physical constraints to individual movement can be extended to individual-level interactions with the same or different species and provides new capabilities for forecasting future responses to novel resource and weather scenarios.

KEYWORDS

biophysical ecology, dynamic energy budget, individual-based model, microclimate, movement ecology, spatial, thermoregulation

1 | INTRODUCTION

Forecasts of individual responses to current and future climates and habitat modification should ideally be based on an explicit understanding of the physiological limits of animals in their environments (Buckley, 2008; Helmuth, Kingsolver, & Carrington, 2005; Kearney & Porter, 2009; Porter, Vakharia, Klousie, & Duffy, 2006; Sears et al., 2016). Exploring how individual traits interact with habitat features and environmental drivers, such as resources and microclimates, offer useful insights into individual behaviour, activity periods and range shifts (Buckley, 2008; Crozier & Dwyer, 2006; Stevenson, 1985b; Vickers, Manicom, & Schwarzkopf, 2011). On short time scales, foraging animals must minimise exposure to extreme environments by exploiting microclimatic variation in their habitats, thereby avoiding physiological hazards such as overheating, cold stress and desiccation (Franklin, Davison, & Seebacher, 2007; Helmuth & Hofmann, 2001; Huey, 1991; Sears, Raskin, & Angilletta, 2011). Potential behavioural responses to such physiological constraints depend on the spatial configuration of resources in relation to microclimates. For example, animals may adjust body temperature while foraging by utilising shade (Shelly, 1982), select oviposition sites by substrate temperature (Davies, Wilson, Coles, & Thomas, 2006) and switch between different activities, such as basking and foraging, to navigate microhabitats (McClure, Cannell, & Despland, 2011) and respond to seasonal changes in habitat suitability (Christian, Tracey, & Porter, 1983). The extent to which an animal risks exposure to extreme environments depends, in turn, on its nutritional and hydration state (Adolph & Porter, 1993; Clissold, Coggan, & Simpson, 2013; Kearney, Simpson, Raubenheimer, & Helmuth, 2010).

By estimating how resources and microclimates drive animal movement, we can build a more realistic picture of animal displacement, habitat use and ecology. Individual-based models (IBMs) are useful tools for exploring how environmental constraints influence animal movement in space and time. For example, they have been used to predict how the spatial distribution of resources drives home range behaviour (Mitchell & Powell, 2012) and how habitat features motivate patch selection (Railsback, Lamberson, Harvey, & Duffy, 1999). In doing so, IBMs can lead to a predictive understanding of the environmental conditions that allow species to invade new habitats and their subsequent shift in distribution (e.g. climate change; Pearson et al., 2006; Randin et al., 2006; see Sears & Angilletta, 2015).

Owing to the multiple constraints imposed on animals, movement models can be complex. Interacting drivers, e.g. resources and cognition (Müller, Fagan, & Grimm, 2011), are often estimated with empirically derived functions (Schurr et al., 2012). Such empirical models are necessarily limited in their generality. We can be more general by capturing and bounding these interactions according to basic physical principles. The fields of metabolic theory and biophysical ecology provide this basis for understanding environmental constraints on animal movement. Metabolic

theory (Brown, Gillooly, Allen, Savage, & West, 2004; Nisbet, Muller, Lika, & Kooijman, 2000) aims to understand how organisms take up energy and matter from their environment and allocate them to the processes of growth, development, maintenance and reproduction. Similarly, the principles of biophysical ecology (Gates, 1980; Porter, Mitchell, Beckman, & DeWitt, 1973) can categorise how these processes are constrained by the thermal and hydration state of an individual. Together, metabolic theory and biophysical ecology provide a complementary understanding of how internal metabolic requirements and external patterns in resources and microclimates constrain movement options (Kearney, Shine, & Porter, 2009; Kearney, Simpson, Raubenheimer, & Kooijman, 2013).

Our approach builds on previous work integrating biophysical ecology and dynamic energy budget (DEB) theory (Kearney, 2013; Kearney et al., 2010) by being explicit about space and movement costs. As such, we aim to link the physical environment and physiological traits with movement-related phenomena, such as home range behaviour and displacement. We outline an energy and mass budget-driven IBM (individual dynamic energy budget movement model; IDEBM) of an ectothermic animal moving in space and time using the IBM protocol (Grimm et al., 2006). We explore how two contrasting movement strategies driven by physiological constraints generate different movement and home range patterns: optimising, where animals move during all thermally available activity times and satisficing, where animals move only when sufficiently hungry based on their metabolism. We do this under two contrasting densities of food and shade.

The model comprises three coupled sub-models that operate simultaneously: (1) a metabolic model of an animal's energy and mass balance, including direct movement costs, based on a general theory of resource uptake and use by organisms (DEB theory; Kooijman, 2010), (2) a transient heat budget model for calculating changes in individual thermal state in response to varying habitat microclimates, and (3) a decision-making model driving movement in space and time. We compare simulated movements to real movement data of 60 adult sleepy lizards for the 2009 breeding season with two major aims:

1. To test whether the IDEBM model can predict movement and home range patterns based on individual physical limits under different food and microclimate constraints
2. To interpret the movement strategy that real individuals in the population use to navigate these movement constraints.

2 | OVERVIEW

2.1 | Purpose

The focal species is *Tiliqua rugosa* (Scincidae), a medium-sized herbivorous lizard from Australia, for which we have detailed field movement

data (see “Data collection” in the appendix and Kerr & Bull 2006 for information on data collection and study site). In the model, the metabolic and thermal state of individuals updates on 2-min time steps to match observed data (see “Data collection” in the appendix and Kerr, Bull, & Cottrell, 2004) as they switch among different activity states of searching (including socialising), feeding (including handling), and sheltering (resting in shade, basking, and “sleeping”) depending on whether in sun, food or shade patches. These behavioural categories define the animal activity budget in space and time over a continuous time scale of the entire breeding season (September to December; 117 days). Individuals follow a correlated random walk (CRW) movement within a 2D model landscape of randomly distributed and clumped food and shade patches interspersed throughout open sun patches. We estimate distributions of shade patches from Light Detection and Ranging (LIDAR) data of the study site by combining a digital surface model and digital terrain model to reflect the spatial arrangement of habitat features, thus providing a realistic picture of the thermal landscape. Hourly microclimates are computed with the NICHEMAPR microclimate model based on daily weather inputs from Australian historic weather data queried from continent wide 0.05° gridded products (Australian Water Availability Project, AWAP [Jones, Wang, & Fawcett, 2009] and a daily wind database [McVicar et al., 2008]). See “NICHEMAPR microclimate model overview” in the Appendix and model overview in supporting material from Kearney, (2013). These hourly predictions are then splined to 2-min intervals and used to update the landscape microclimate at each time step. See Figure 1 for input pathways of microclimate data. Functions for the energy and mass budget calculations are part of the R (R Development Core Team, 2015) package “NICHEMAPR” (<https://github.com/mrke/NicheMapR>). Metabolism is modelled using the function “DEB.R” and a transient heat budget “onelump_varenv.R” driven by the environmental output

from the “microclimate” function updates the individual thermal state (<https://github.com/darwinanddavis/MalishevBullKearney>).

The decision-making IBM (Appendix 1 in Supporting information) is implemented in Netlogo (Wilensky, 1999) and simulated from R. The energy and heat budget models (Appendix 2 in Supporting information) described above are first implemented in R, then integrated with the IBM simulations using the “RNETLOGO” package (Thiele, Kurth, & Grimm, 2012). The detailed breakdown of the energy and mass budget is presented in Appendix 3 in Supporting information. Italicised text denotes DEB and NICHEMAPR variables and parameters, e.g. *E*, and code typeface denotes IBM simulation parameters, e.g. *reserve-level* and procedures, e.g. *Feeding*.

3 | ENTITIES, STATE VARIABLES, AND SCALES

The model has three entities—individuals, habitat and microclimate—simultaneously driven by the energy budget (DEB), the heat budget (NICHEMAPR), and the decision-making model (IBM).

3.1 | Energy budget model

The energy budget model uses individual morphology and physiology data with theory-driven principles of energy and mass balances to update the internal metabolic state of the animal, including food processing and intake rates, somatic maintenance and movement costs, and growth and reproductive rates. We incorporate the core assumptions and basic rules of DEB theory (see Appendix 3 in Supporting information) as a coupled energy and mass budget model (see Figure 3 in Kearney & Porter, 2009) into an IBM that updates the individual

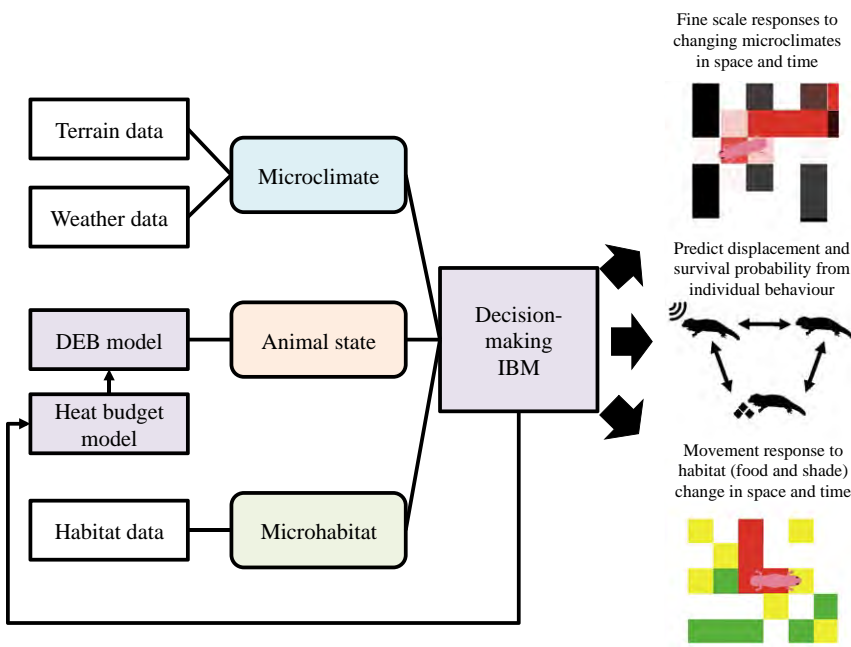


FIGURE 1 Schematic of data and model inputs of the individual dynamic energy budget movement model. Examples of weather data: monthly to annual temperatures microclimate; Microclimate: local solar and infrared radiation temperature, ground and air temperature (Table 2); dynamic energy budget model: See Tables 1 and 4; Heat budget model: See Table 2; Habitat data: food and shade patches (Table 3). The dynamic energy budget and heat budget models update with the time steps of the decision-making individual-based model to form feedback loops. All weather and habitat data are modeled on the sleepy lizard habitat (139°21' E, 33°55' S). Animal data are for the adult sleepy lizard

internal state on 2-min time steps. This then drives movement and changes in metabolism (including direct movement costs) to generate changes among activity states and the overall activity budget, home range emergence, and habitat use. It thus provides a way to compute the animal's motivational state for movement (hunger, reproduction) and predict fitness consequences (growth, reproduction, condition) of different movement strategies. Table 1 shows the DEB parameters estimated using the "covariation method" (Lika et al., 2011) from animal data and Appendix 3 in Supporting information shows a summary of DEB procedures.

3.2 | Heat budget model

The heat budget model computes heat exchange between animal and environment based on morphology (e.g. body mass, length, surface area, and solar reflectance), physiology (e.g. metabolic rate, rates of food intake and processing), behaviour (e.g. foraging temperature thresholds), and environmental conditions (e.g. ground and air temperature, wind speed, solar radiation, and infra-red radiation) (Kearney & Porter, 2004). Following Porter et al. (1973), we compute body temperature T_b as the sum of the steady y_s and transient y_t thermal state, $T_b = y_s + y_t$

$$T_b = \frac{j}{k} + \left(T_b - \frac{j}{k}\right) e^{-kt} \text{ and } \frac{\delta T}{\delta t} = j - kT_b, \quad (1)$$

where $j = (Q_{\text{sol}} + h_c A_{\text{conv}} T_{\text{air}} + h_r A_{\text{rad}} T_{\text{rad}})/C$, $kT_b = T_b(h_c A_{\text{conv}} + h_r A_{\text{rad}})/C$, k is a time constant, Q_{sol} is the total solar radiation absorbed, A_{conv} and A_{rad} are the surface areas for convective and radiative heat transfer, respectively, C is the thermal capacitance (specific heat capacity \times mass), h_c is the convection coefficient, and h_r is the radiation coefficient (approximated in our model by a Taylor series expansion $4\epsilon\sigma\left(\frac{T_b + T_{\text{rad}}}{2}\right)^3$ with emissivity ϵ and Stefan-Boltzmann constant σ). Note, for simplicity, we here neglect metabolism, evaporation, and conduction, but they can be incorporated if required (Porter et al., 1973). The time constant $\frac{1}{k}$ accounts for the response time of T_b between steady and transient states that influences heat transfer through the animal depending on individual thermal mass. See Table 2 for individual parameters and variables, Appendix 2 in Supporting information for detailed heat budget R code, Kearney et al. (2010) for complementary ways to integrate biophysics with energetics (DEB theory), and Kearney et al. (2013) for applying the combined framework in a spatially implicit manner with a steady-state heat budget model to the Cunningham's skink, *Egernia cunninghami*.

TABLE 1 Individual variables and parameters of the DEB (dynamic energy budget) model (Kooijman, 2010) parameterised for the sleepy lizard, *Tiliqua rugosa*. Parameters are estimated from available animal data (Table 4). Dimensions: –, dimensionless; J, Joules; L, structural length; t, time. Units: d, days; cm, centimetres. Square [*] and curly {*} parentheses denote parameters per volume and surface area, respectively; dot accents denote rates

Parameter	Value	Dimension	Unit	Description
\dot{p}_X	330.04	J/t	d	Flux for food uptake from environment to individual
\dot{p}_A	280.53	J/t	d	Flux for food assimilated to energy, where $\{\dot{p}_{Am}\}$ is the maximum assimilation rate ($f = 1$).
κ	0.84	–	–	Kappa rule of energy allocation
\dot{p}_C	232.51	J/t	d	Energy flux mobilised from reserve. $\kappa\dot{p}_C$, energy allocated to soma; $(1 - \kappa)\dot{p}_C$, energy allocated to maturity
\dot{p}_M	117.56	J/t	d	Flux for somatic maintenance
\dot{p}_G	78.71	J/t	d	Flux for growth
g	1.95	–	–	Energy invested into growth (per maximum reserve $[E_m]$)
\dot{p}_J	12.49	J/t	d	Flux for maturity maintenance
\dot{p}_R	23.75	J/t	d	Flux for maturation or, once fully matured, for reproduction
ν	0.03	L/t	cm/day	Energy conductance
r	0.00017	t^{-1}	d	Specific growth rate (of structure)
$[E_G]$	7,772	J/L^3	cm^{-3}	Cost of structural tissue
$\{F_m\}$	6.5	L^2/t	cm^2/day	Maximum surface-specific searching rate of food
κ_X	0.85	–	–	Energy assimilation efficiency
κ_R	0.95	–	–	Reproduction efficiency
$\{\dot{p}_T\}$	0	$J L^2/t$	cm^2/day	Flux for surface-area specific somatic maintenance
\dot{k}_j	0.002	t^{-1}	d	Coefficient for rate of maturity maintenance
E_H^b	102,980	J	–	Maturity threshold at birth
E_H^p	249,580	J	–	Maturity threshold at puberty
E_R	0	J	–	Reproduction buffer

3.3 | Decision-making IBM

The decision-making IBM simulates CRW movement in a 2D model landscape of randomly distributed food and shade, where environmental conditions update the coupled energy and heat budget to define the individual internal state and thus inform future behaviour and movement potential. Individuals follow either an optimising or satisficing movement strategy and move only when within their physiological limits (T_{lower} and T_{upper} , Table 2): optimising animals move during all available activity hours, whereas satisficing animals move only when hungry (gut fullness level is <75% [Kearney et al., 2013]) and thus avoid socially motivated movement. We choose these strategies for their relationship with decision-making and animal behaviour studies, i.e. foraging under environmental extremes is risk-taking and involves trade-offs. Individuals switch between three activity states depending on their current state and whether in food, sun, or shade: searching for food or shade (*Searching*), consuming food (*Feeding*), or sheltering in shade (*Resting*). For example, under either strategy, being in open sun while *Searching* or *Feeding* can push the animal outside its physiological limits (T_{lower} and T_{upper}), forcing it to seek refuge in shade.

Optimising animals have the additional socialising activity state, which involves the same CRW movement, but motivated by social and territorial requirements categorised within *Searching*. Socialising is included in this strategy as it can contribute to dispersal potential and behavioural adaptation within an animal's overall activity budget (Bateman, Lewis, Gall, Manser, & Clutton-Brock, 2015; Kays, Crofoot, Jetz, & Wikelski, 2015; Spiegel, Leu, Sih, & Bull, 2016; Wang & Grimm, 2007).

TABLE 2 Individual variables and parameters of the transient heat budget model. Dimensions: –, dimensionless; C, Celsius; J, Joules; kg, kilograms; m, metres; s, seconds; t, time; W, watts

Parameter	Dimension	Description
T_b	°C	Core body temperature
T_{lower}	°C	Lower body temperature bound of activity range
T_{upper}	°C	Upper body temperature bound of activity range
σ	°C	Stefan–Boltzman coefficient
cp	J/kg	Specific heat of flesh
$emis$	–	Emissivity of skin
Fo_e	–	Configuration factor of animal to absorb infrared radiation
ρ	kg/m ³	Density of animal mass
abs	–	Solar absorptivity of animal
Q	W	Heat fluxes
y	°C	Thermal state of animal: steady y_s and transient y_t
j	°C	Temperature constant
k	1/s	Time constant
C_1	–	Dimensionless constant
e^{-kt}	–	Dimensionless rate of T_b change

Additional traits include perception range for locating food and shade patches and activity counters for time spent searching, feeding, and sheltering. See Table 3 for individual-based parameters and variables.

3.4 | Habitat

The habitat variables are *food*, *shade* and *sun* patches distributed in the environment (Table 3). Food is either a small or large food item per open sun patch and is either sparsely or densely distributed under the two movement strategies. Food intake by individuals is determined by handling time (patch residence). Shade is single patches and estimated from vegetation inputs from LIDAR data of the study site.

3.5 | Microclimate

Patches are either shade or open sun (including food) determined by microclimate inputs of air temperature, relative humidity, ground temperature, wind velocity, solar zenith angle and solar and infrared radiation from microclimate input data of the study site. We calculated microclimates from Australian historic weather data using the NICHEMAPR microclimate model (see model overview in supporting material from Kearney, 2013), which we pre-computed hourly, then interpolated (splined) to 2-min time steps during the simulation with the R function “approxfun” from the STATS package (Chambers, Becker, & Wilks, 1988).

3.6 | Scales

One patch is one cell on the model spatial grid (2 m²; Table 3). Simulations run on 2-min time steps. Initial microclimate inputs are initialised hourly then projected (splined) to 2-min time steps.

4 | PROCESS OVERVIEW AND SCHEDULING

Individuals are motivated both to find food (X) and to avoid environmental extremes. Food may be small (3 kJ) or large (6 kJ) items with one (2 min) or two (4 min) handling time steps, respectively. These energy values reflect the stomach-emptying rate specified by DEB theory following the Holling Type II functional response (Holling, 1959). Energy reserves change on each time step as dictated by the reserve (E) dynamics of the DEB model relative to body temperature (T_b) (influenced by microhabitat/microclimate) and by whether or not it is feeding in that time step. Movement incurs a direct movement cost estimated from O₂ expenditure rates for a similar-sized ectotherm (John-Alder, Garland, & Bennett, 1986) and converted to maintenance costs per unit of body mass generated by the DEB model (O₂ per gram converted into Joules). The reserve level then influences the dynamics of fitness outputs, such as growth, development, and reproduction (see Appendix 3 Supporting information for summary of DEB parameters and primary metabolic pathways). Individuals also regulate their body temperature within their thermal constraints (Table 2) on each 2-min time step according to their current location in space, i.e. shade vs.

TABLE 3 State variables and parameters of model individuals, habitat, and microclimate. Dimensions: –, dimensionless; C, Celsius; J, Joules; m, metres; s, seconds; t, time; T, temperature; W, watts. As in 2. Entities, state variables and scales

Entity	Variable/ parameter	Notation		Dimension (unit)	Description
		DEB	IBM		
Individual	Reserve density	[E]	Reserve-level	J cm ³	Dynamic energy budget (DEB) individual state variable that relates to nutritional state and contributes to part of the biomass. Dynamics of reserve flux is determined by the kappa (κ) rule of energy allocation that controls energy allocation to essential metabolic processes, such maintenance, growth, maturity, and reproduction. $[E_m]$ is maximum reserve density. See Equation 4 in Appendix 3 in Supporting information
	Structure	V	–	cm ³	A DEB state variable proportional to physical length that contributes part of the biomass. Structure increases (growth) based on flux of mobilised reserve. See Equation 11 in Appendix 3 in Supporting information-Growth is modelled by the DEB growth equation, the parameters of which are estimated from individual traits (e.g. snout to vent length (SVL)). See Table 4 for empirical data used to parameterise the DEB model
	Maturity	E_H	–	J	A DEB individual variable that determines the maturity stage of animal. The case study model considers a mature adult, so $E_H = E_H^p$
	Movement strategy	–	Optimising Satisficing	–	An individual-based model (IBM) parameter defining the movement strategy of the individual in space. Optimising animals include an additional socialising activity state
	Gut level	E_{sm}	gutfull	J cm ³	A DEB variable representing stomach capacity that determines the level of food in the animal gut. Parameterised on the Cunningham's skink (Kearney, 2012)
	Vision	–	min-vision	Patch (m ²)	An IBM parameter defining the visual scope of the individual and its encounter probability of food and shade patches in space. Min-vision refers to the normal visual scope (10 m) (Auburn et al., 2009)
	Functional feeding response	f	energy-gain	–	A DEB individual parameter that defines food (X) intake per encounter rate with food patches. $f(X) = \frac{X}{X+K}$, where $K = \frac{(\beta_{sm})}{\kappa_X(E_m)}$ the half saturation coefficient, following (Holling, 1959) (see Table 1 for K)
Habitat	Food	X	Yellow patch: small food Green patch: large food	Patch (m ²)	Food items vary in size (bites) per food patch. Small and large food items take one (2 min) or two (4 min) time steps, respectively (handling time). Food and sun patches represent similar microclimates
	Shade	–	Black patch	Patch (m ²)	Shade patches are distributed randomly in the model landscape, reflecting typical spatial arrangement in nature
Microclimate	Solar radiation	SOLR	–	W/m ²	A NICHEMAPR variable. The model environment is loaded with these data prior to simulation runs, updated hourly within NICHEMAPR, and splined to 2-minute time steps
	Local air temperature	TALOC	–	T (°C)	A NICHEMAPR variable. Input as per solar radiation
	Infrared radiation	IR	–	W/m ²	A NICHEMAPR variable. Input as per solar radiation
	Relative humidity	RHLOC	–	%	A NICHEMAPR variable. Input as per solar radiation
	Soil temperature	TS	–	T (°C)	A NICHEMAPR variable. Input as per solar radiation
	Local wind speed	VLOC	–	m/s	A NICHEMAPR variable. Input as per solar radiation

sun patch and the time of day per month. See Figure 1 for data inputs, Figure 2 for schematic of simulation runs, and Appendix in Supporting information 1 for IBM simulation code.

5 | DESIGN CONCEPTS

5.1 | Basic principles

The environmental conditions (microclimatic values in the extremes of available shade), animal traits (DEB and the heat budget model) and resource densities (food and shade) are the three model inputs. The individual executes its movement decisions—searching for food or shade (*Searching*), consuming food (*Feeding*), or sheltering in shade (*Resting*) under either an optimising or satisficing movement strategy—in response to changes in these types of input, generating spatial movement patterns and fine-scale behavioural responses to changing constraints (see Figure 1).

5.2 | Emergence

Activity and home range patterns emerge from the two movement strategies in space and time in response to microclimate and food constraints. We interpret individual activity states and home range emergence in space using the 95% kernel utilisation distribution (UD)

$$UD'(x, y|t_i) = \frac{UD(x, y, t_i)}{\int_{x', y'} UD(x', y', t_i)}, \quad (2)$$

where x , y and t_i are x coordinates, y coordinates, and time for the i th coordinate relocation, respectively. Individual T_b , including the rate of T_b change, and current metabolic state of the animal updates the individual internal state per model time step to drive future movement decisions and thus home range emergence. For example, the individual will seek shade or forage depending on the external

environmental temperature and whether within its activity temperature range (T_{lower} and T_{upper}). Based on how the external environment influences the internal individual state, this leads the individual to either displace from its current location in search of shade or food or remain in a resting state in shade to avoid environmental extremes, thus expanding or contracting its home range area.

5.3 | Adaptation

The internal metabolic and thermal state drives individual responses to environmental change. For example, if environmental conditions are outside the specified range for emergence or activity, the animal will remain in its shelter. Within these limits, animals can bask by actively seeking sun patches when attempting to reach a preferred basking temperature, or search for food, feed, or socialise when within their T_{lower} and T_{upper} activity range limits. Individuals must regulate their T_b in response to changing microclimates by adapting their movement on fine scales to their current physiological state (mass, energy reserve), the level and availability of shade, and photoperiod. For simplicity, we assume no burrowing behaviour.

5.4 | Fitness

The DEB model computes the trajectory of the life history at any stage in the life-cycle and thus defines potential fitness components, such as growth or fecundity for a given simulation.

5.5 | Prediction

By simultaneously computing individual movement from thermal and resource limits of the habitat and the metabolic drive to move based on temperature and hunger levels, the model predicts movement constraints from purely individual physiological limits.

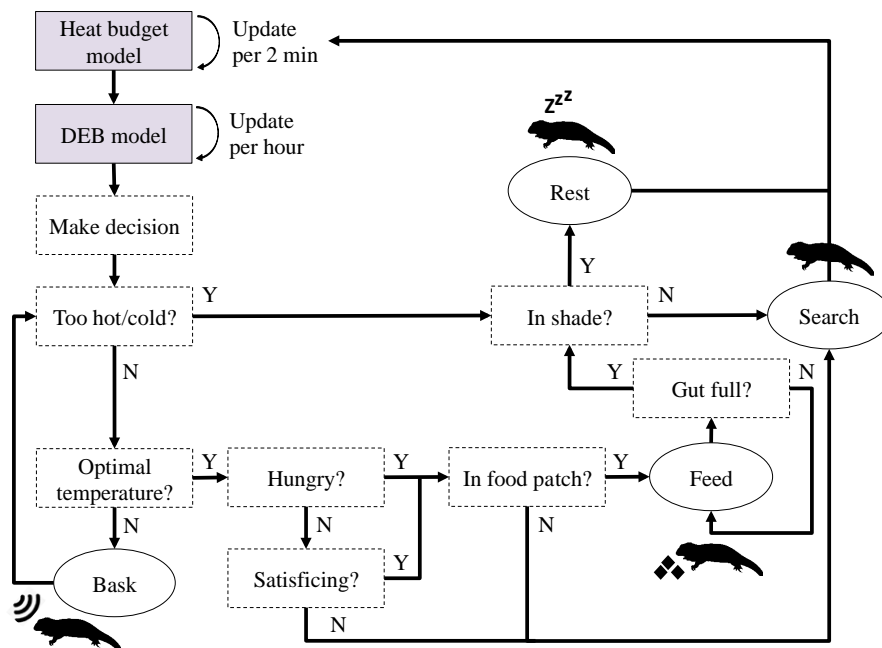


FIGURE 2 Schematic of decision-making individual-based model simulation runs. Solid boxes are processes, dashed boxes are individual decisions, and ellipses are individual actions. Searching refers to either searching for food, shade, or socialising, depending on the current thermal or metabolic state or movement strategy of the animal. Hungry refers to whether the gut fullness threshold is <75%

5.6 | Sensing

Individuals are aware of their habitat (food and shade) in space and time within a defined visual range (*min-vision*; Table 3), allowing them to gravitate towards food or shade patches that lie within this range depending on their current activity state.

5.7 | Stochasticity

Individual decisions are to some extent random (e.g. which direction to turn) following correlated random walks (CRW), which assume the least about any preferences for habitat features. This stochasticity generates different activity budgets under different movement strategies and resource distributions. When food or shade patches fall within the vision range, the individual will orientate and move itself directly towards the appropriate patch given the current activity state, i.e. Searching or Resting.

5.8 | Observation

The model produces individual outputs for body temperature (T_b), rate of change in T_b , activity budget in time and space (time spent and spatial coordinates of different activity states), accumulated direct movement costs, accumulated wet mass (structure, storage, food and reproductive mass), gut fullness and home range polygons for both movement strategies.

6 | DETAILS

6.1 | Initialisation

All animal data are based on the adult sleepy lizard, *T. rugosa*. Activity temperature range for *Searching* is 26°C and 35°C for the lower and upper bounds, respectively (Table 2), and basking temperature is 14°C (Pamula, 1997). Vision range (*min-vision*) is 10 m (Table 3) (Auburn, Bull, & Kerr, 2009). Table 4 details the parameters for initialising the DEB model for *T. rugosa*. We set up the IDEBM model to simulate real movement data of location tags every 10 min and movement steps, body temperature (T_b), and energy reserves recorded every 2 min of 60 adult sleepy lizards in the 2009 breeding season (September to December).

Individuals are initialised as adults at the onset of maturity and begin in a shade patch (*Resting*) in the centre of the landscape with maximum reserve (*Maximum-reserve*). Initial body temperature (T_b) depends on the user-defined location in space and time of year. Minimum and maximum activity temperature range (°C), basking temperature (°C), body mass (g), and vision range (m) are user-defined. We simulated an individual in a habitat of randomly distributed food and shade patches for 117 days from September 5, 2009. Simulations were repeated 100 times using a seeded habitat arrangement for (1) the optimising vs. satisficing strategies and (2) sparse (1,000) vs. dense (100,000) food and shade distributions. We then compared movement pattern simulations with home ranges of sleepy lizard GPS data for this time period.

TABLE 4 Organism data for parameterising the standard dynamic energy budget model of *Tiliqua rugosa*. Unit: d, days; g, grams; K, Kelvin. All data are from Kearney, M. R., Munns, S. L., Moore, D., Malishev, M. and Bull, C. M., unpubl. data, (http://www.bio.vu.nl/thb/deb/deblab/add_my_pet/entries_web/Tiliqua_rugosa_res.html), except life span, which is from (Snider & Bowler, 1992)

Parameter	Value	Unit	Description
a_b	150	d	Age at birth at f (age 0 is at onset of embryo development)
T_{ab}	302.25	K	Temperature for a_b
a_p	1642.5	d	Time since birth at puberty at f
T_{ap}	302.25	K	Temperature for a_p
a_m	7628.5	d	Life span at f (accounting for ageing only)
T_{am}	296.35	K	Temperature for a_m
L_b	16.5	cm	Snout to vent length at birth at f
L_p	23	cm	Snout to vent at puberty at f
L_i	32.8	cm	Ultimate snout to vent length at f
W_b	29.7	g	Dry weight at birth at f
W_p	54	g	Dry weight at puberty at f
W_i	215.1	g	Ultimate dry weight at f
R_i	0.0024	d ⁻¹	Maximum reproduction rate at f (for individual of max length)
T_{Ri}	296.35	K	Temperature for R_i

7 | INPUT DATA

7.1 | Habitat

The habitat represents an arid, terrestrial environment in South Australia (139°21' E, 33°55' S), 1.5 × 1.5 km. Grid cells in the model landscape are 2 m wide.

7.2 | Microclimate

The habitat is a mosaic of sun and shade patches (sparse or dense) that animals, when simulated to enter either patch type, are exposed to the respective sun or shade microclimate for the study site throughout the breeding season (September to December, 2009). We estimated distributions of shade patches from the LIDAR data of the study site and calculate hourly microclimates from the NICHMAPR microclimate model, using continent-wide weather data.

8 | SUBMODELS

8.1 | Activity budget

Individuals switch between three separate activity states that encompass the fundamental behavioural repertoire: *Searching* for food, *Feeding* (including handling), and *Resting* (sheltering, seeking shade, and basking). For example, less time spent sheltering relative to feeding could imply that the animal is malnourished or lives around patchy resources. Emergent individual behaviour generates transition

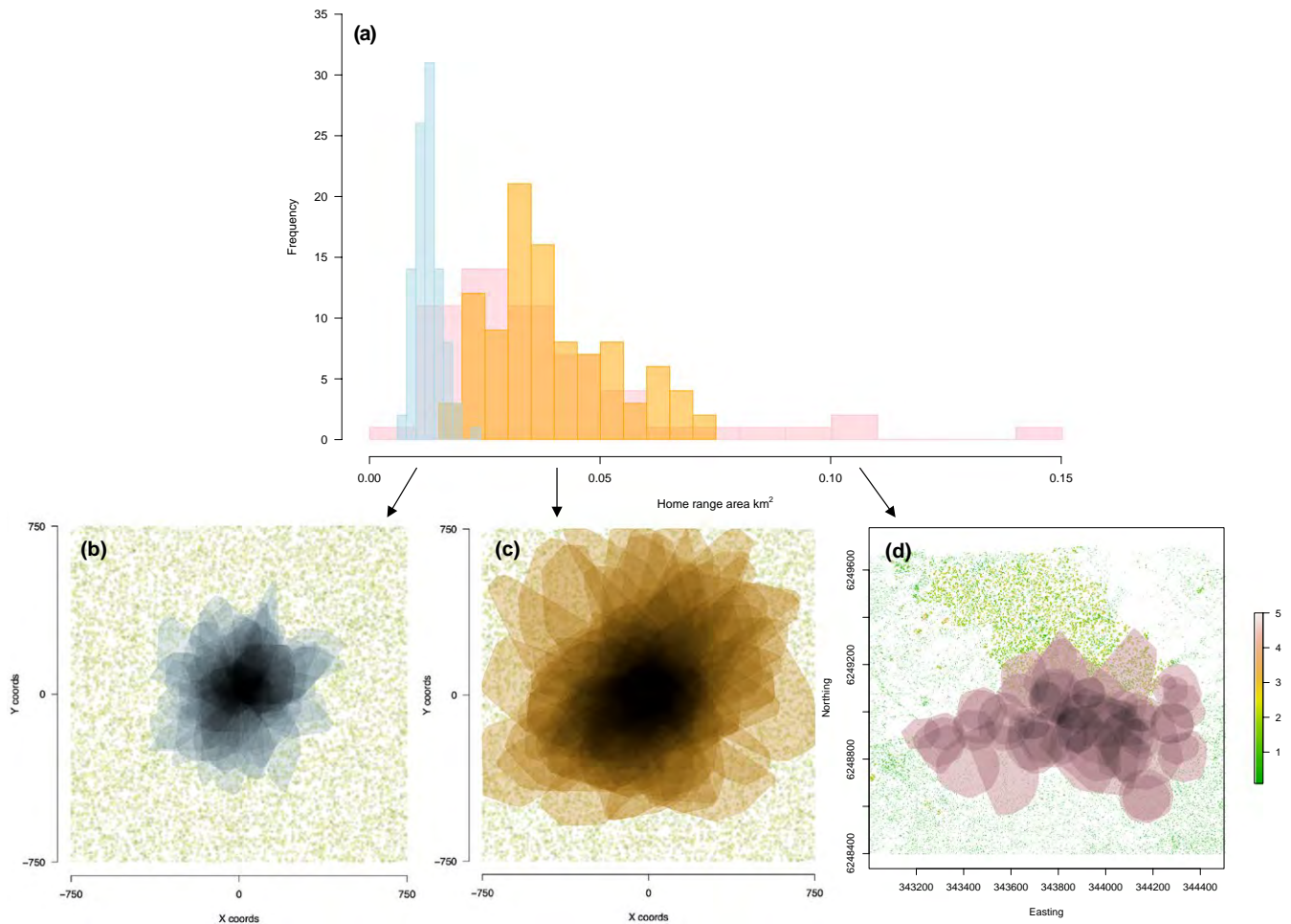


FIGURE 3 (a) Distributions of home range area (km^2) of real (pink) and seeded simulated optimising (orange) and satisfying (blue) movement strategies under dense resource distribution (food and shade). Home range polygons in space showing overlap of seeded simulated (b) satisfying and (c) optimising individuals and (d) real individuals. Home ranges in (d) appear more scattered due to different starting locations of real animals, whereas (b) and (c) have seeded starting locations in the centre of the landscape. The vegetation layer in (d) is generated from Light Detection and Ranging data of the habitat site, showing the thermal mosaic of the landscape

probabilities between activity states and thus a global state space model. Optimising animals have the extra activity state of socialising.

9 | RESULTS

9.1 | Does the model capture realistic home range area and behaviour?

We used a metabolic theory-based movement model defining the internal energy and mass budget to drive movement decisions and generate activity budgets and home range emergence in response to external environmental constraints of food and microclimates explicitly defined in space and time. Using satisfying and optimising strategies as proxies for minimum and maximum potential movement, the IDEBM model produced distributions of home range size which overlap with that of the wild population (Figure 3). Mean home range area for real animals (0.038 km^2) was significantly greater than simulated satisfying animals (0.0126 km^2 , $t_{54,6} = 7.0376$, $p < .001$), but not different from simulated optimising animals (0.0397 km^2 , $t_{69,5} = 0.39715$) (Figure 3). This implies

that actual lizard movement extends beyond basic behaviours of feeding, searching, and resting to include extra movement relating to socialising (Figure 4b). Some home ranges of real animals were larger than those from any of the two simulated movement strategies, but this portion of the total number of observed animals was only 10% ($n = 6$). Further, the mean home range area of observed animals is closer to that of either simulated movement strategy than the maximum observed home range area. Under an optimising strategy that allows socially motivated movement, individuals covered more ground and thus explored more food and shade patches within a similar time period compared to satisfying ones (Figure 5c–d). Animals were also able to successfully negotiate different habitat arrangements, as shown by similar home range sizes between sparse and dense resource distributions (Figure S1).

9.2 | How does movement strategy shape activity budgets?

From individual-based decisions based on the internal energetic and thermal state of the animal in response to a spatial resource

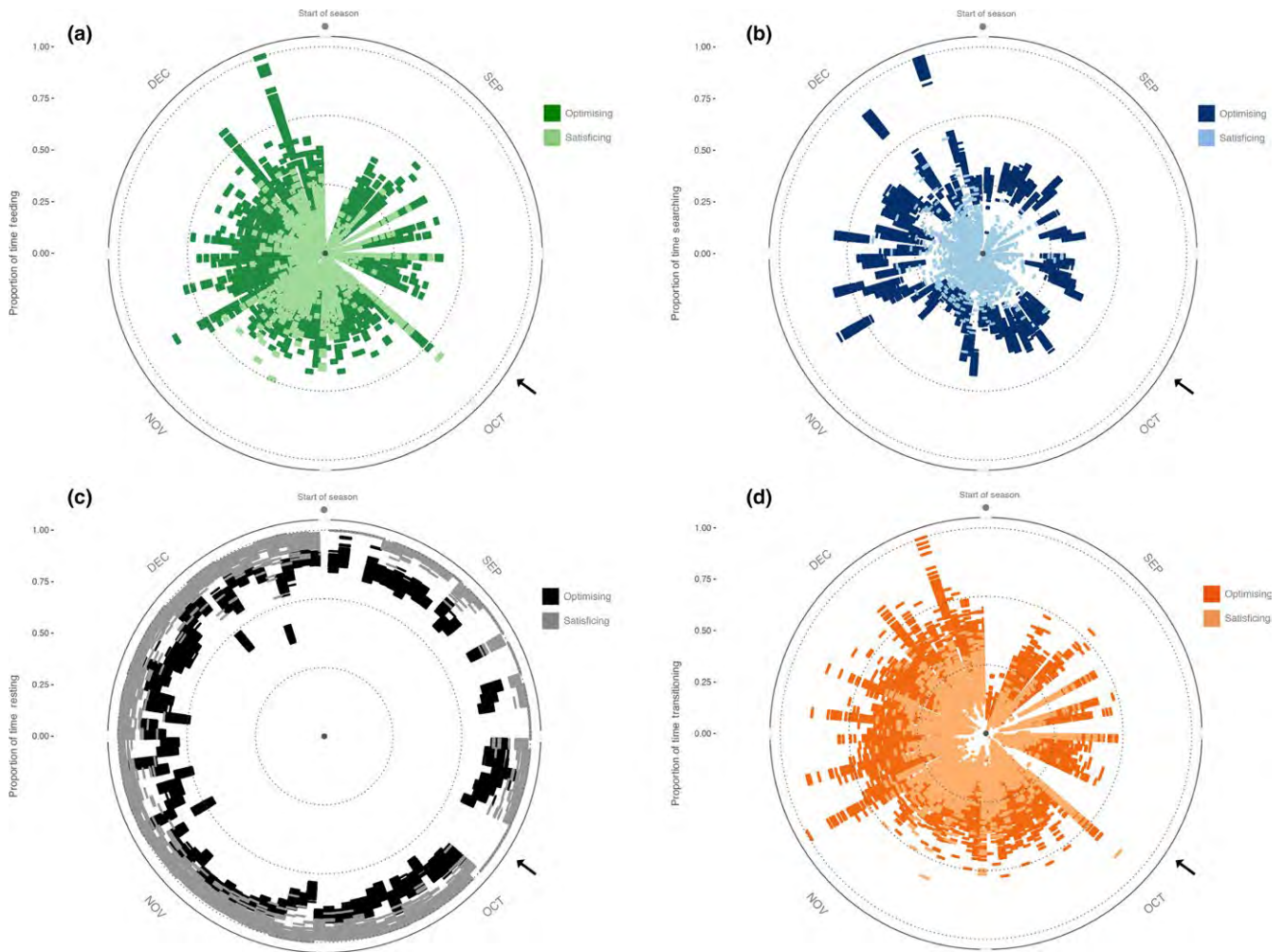


FIGURE 4 Activity budget for all optimising and satisficing animals throughout the breeding season showing proportion of time spent (a) feeding, (b) searching, and (c) resting, as well as (d) proportion of number of transitions between activity states. Radius = time spent in activity state; circumference = days throughout the breeding season. Black arrows indicate a 5-day period where environmental conditions were not conducive to activity, so animals spent this time resting in shade

landscape, home range vertices show that optimising individuals under high resource distribution covered 1.2-fold more area (km^2) feeding than either searching or resting. Optimising animals spent on average 4.1-fold more time searching, 2.7-fold more time feeding, and 1.8-fold more time transitioning between activity states than did satisficing animals (Figure 4). As expected, the largest difference in activity between movement strategies was for resting; satisficing animals, who spent 1.2-fold more time resting than optimising animals, were restricted from any non-feeding activities, i.e. socialising. Optimising animals spent 10.5-fold more time searching and 47.9-fold more time resting than feeding. Conversely, satisficing animals spent 6.9-fold more time searching and 149-fold more time resting than feeding.

9.3 | How does movement potential affect individual metabolic outputs?

Movement was, on average, 1.4-fold more costly for maximum (optimising) over minimum (satisficing) movement potential due to

extra overall time engaging in non-feeding movement (Figure 6a). The IDEBM model predicted relatively minor impacts on the energy budget of the two movement strategies: structure, wet mass storage, converted food mass, and reproductive organ wet mass of optimising animals were, on average, 0.0004%, 0.0008%, 0.0009%, and 0.0023% (g) lighter after the breeding season than in satisficing animals, respectively (Figure 6b).

9.4 | Does the individual heat budget model capture realistic thermal changes and costs?

We found the upper and lower T_b limits per hour of the day for the different simulated movement strategies encompassed those of the wild population throughout the breeding season, while average hourly simulated T_b varied from observed by $\pm 5^\circ\text{C}$ (cf. Figure 7a–b). An example of the fine scale changes in T_b as the individual enters and exits shade patches across the day is shown in Figure 7. Rates of T_b change for simulated minimum and maximum movement potential showed a similar range to those of the real animals (Figure S2).

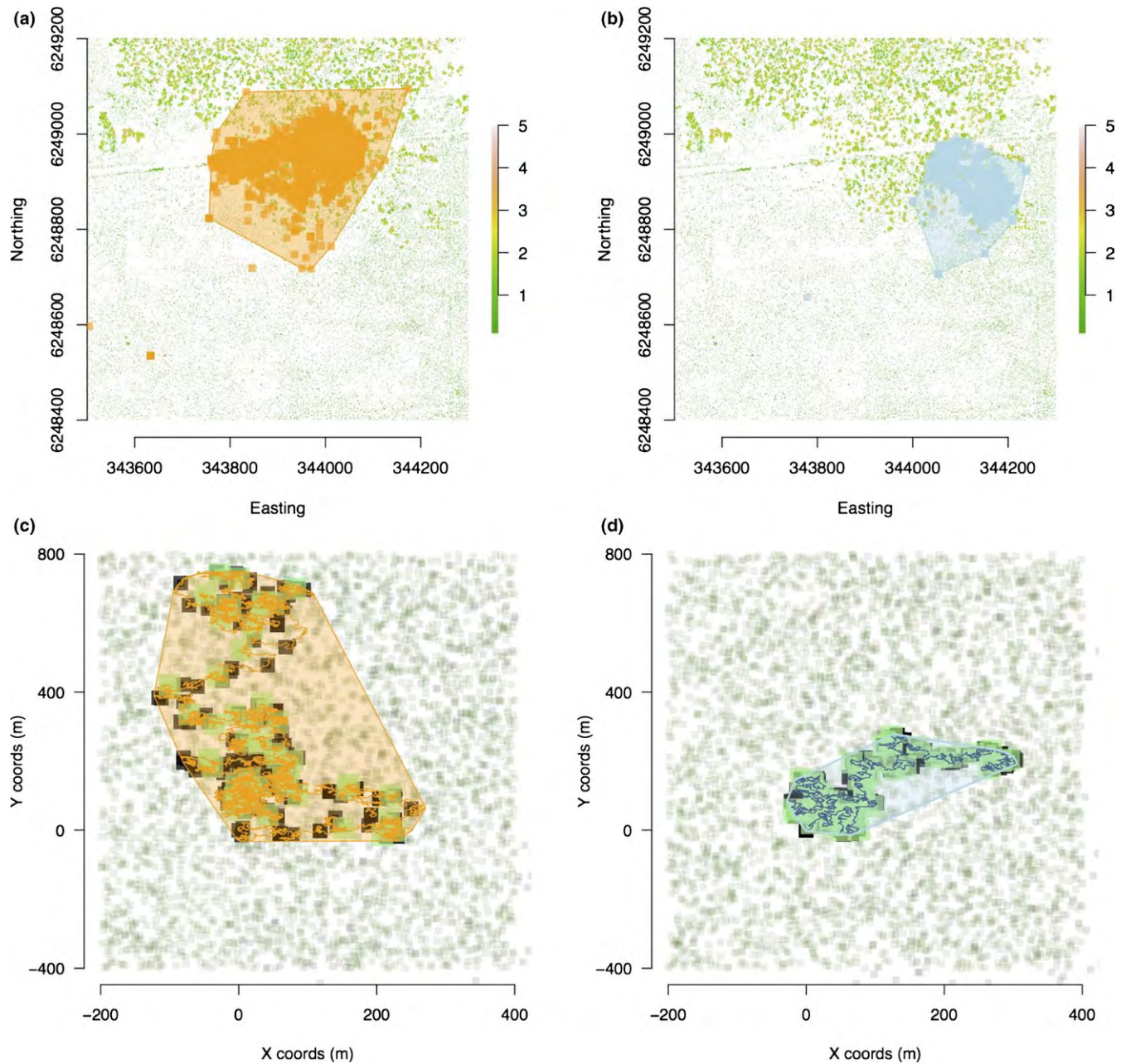


FIGURE 5 Movement path and home ranges of real vs. simulated sleepy lizards. (a) Individual #11885, a real sleepy lizard showing active movement and (b) individual #11533, a real sleepy lizard showing passive movement, throughout the breeding season. (c) A random simulated optimising individual representing the maximum potential movement and (d) a random simulated satisfying individual representing the minimum movement necessary throughout the breeding season based on its physiological limits. (c–d) green = food patches, black = shade patches, and polygons represent home ranges. Patch size in simulations represents time elapsed on patch

10 | DISCUSSION

We built an individual-based spatial movement model driven by mechanistic models of heat exchange and metabolism to predict movement and home range patterns under different food and microclimate constraints. Our aim was to interpret how animals navigate these movement constraints from interacting internal (physiology and metabolism) and external (resource and weather) cues under different movement strategies to capture habitat use of the wild population.

Simulated average home ranges under the optimising strategy closely approximated real home ranges throughout the breeding season (Figure 3). Therefore, our movement model driven from bottom-up physiological and metabolic consequences was able to provide biologically realistic predictions. Given that real animals move significantly more than predicted by the simulated satisfying strategy, our results imply that sleepy lizards are exploiting available thermally suitable time for activities above and beyond what is needed for feeding (Figure 3). This is consistent with field studies of sleepy lizards

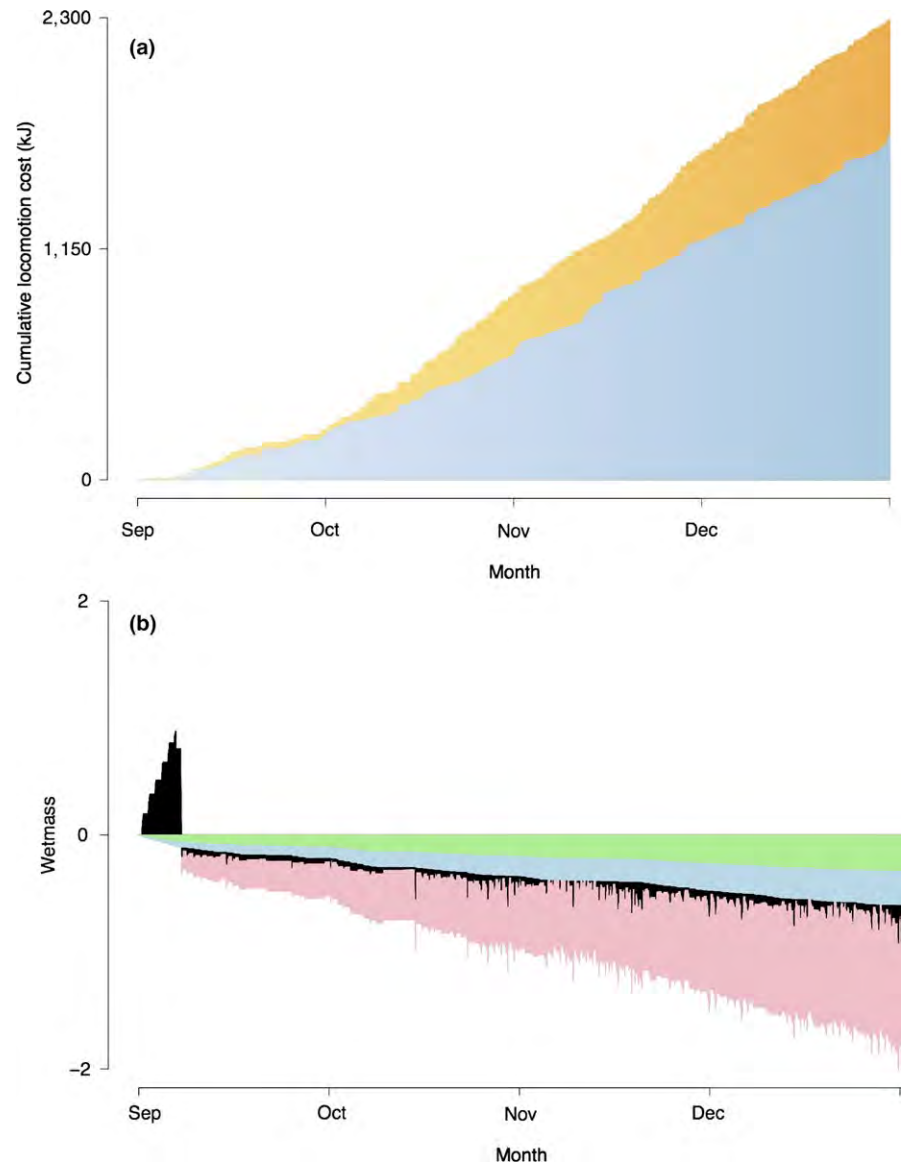


FIGURE 6 Energetic outputs showing differences in maximum (optimising) and minimum (satisficing) potential movement. (a) Cumulative movement costs (kJ) for a random simulated optimising (orange) and satisficing (blue) individual throughout the breeding season. (b) Difference in mean structural volume ($\text{g}^{-1} \text{cm}^3$; green), wet mass storage (g; blue), converted food mass (g; black), and reproductive organ wet mass (g; pink) between optimising and satisficing movement strategies throughout the breeding season

showing that males in particular engage in extensive movements associated with mating and social behaviour (Kerr & Bull, 2006).

The motivations of animals to trade-off available time for different activities are diverse e.g. growing vs. mortality risk (Stamps, 2007; Werner & Anholt, 1993), rapid habitat change (Fahrig, 2007), and the interplay between the internal state and external environmental cues (Clobert, Le Galliard, Cote, Meylan, & Massot, 2009; Schick et al., 2008; Shaw & Couzin, 2013). Animals face movement trade-offs depending on how food and microclimates change in space and time on fine scales (McClure et al., 2011; Porter et al., 1973; Stevenson, 1985b). By adjusting behaviour and activity windows to exploit different thermal landscapes, animals can better regulate their body temperature (Sears et al., 2011; Vickers et al., 2011; Villén-Pérez, Carrascal, & Seoane, 2013) and better adapt to fine-scale environmental change. The 95% home range vertices we computed for each activity state showed that simulated patch use from searching for food and feeding covered the most ground because when food is abundant, i.e. under high resource distribution, animals can easily find and move to nearby food patches.

Animals can then use food patches as stepping stones to find more food; in contrast, more patchy food distribution lowers the chance of finding and thus moving to food patches. Therefore, space use by simulated animals when feeding required more directional movement and was less random than when searching, including socialising. More time spent feeding suggests that, under physiological constraints, foraging drives movement over socialising.

Simulated shade-seeking behaviour, including retreating to shade, covered less area because resting animals are more stationary and displace less than foraging ones. This result is likely due to the time costs of different activities. For example, animals heat up and cool down over much shorter time intervals than those involved in searching for and handling food. That is, they may have to continually leave a food patch to cool down in a shade patch in hot weather. Therefore, thermal extremes can impose significant overhead costs to foraging time. For example, active lizards in open patches can spend up to 20-fold more time in foraging than non-foraging behaviour (Wilson & Lee, 1974). We found simulated animals spent more time exposed to thermal

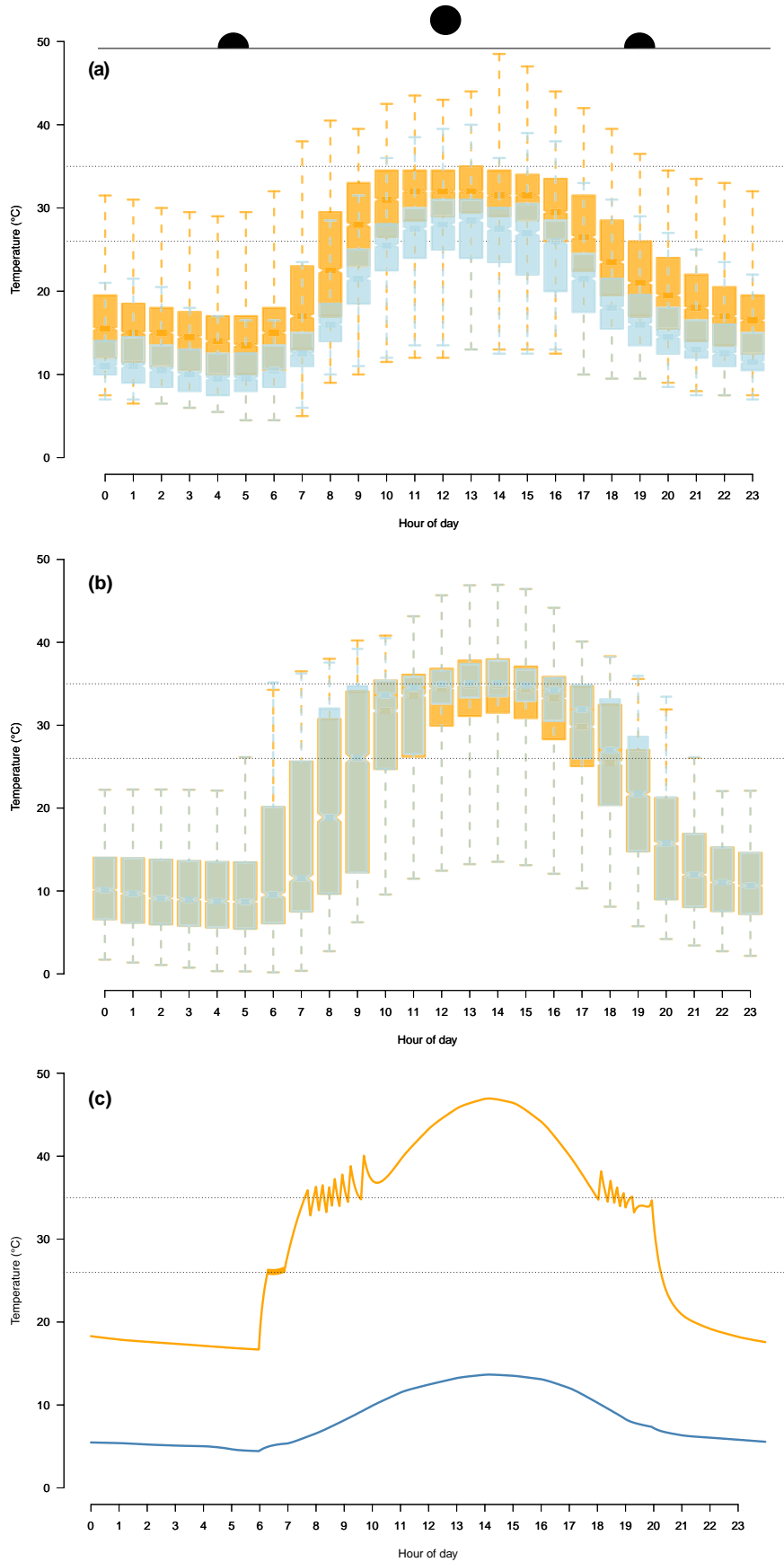


FIGURE 7 (a) Hourly T_b for individual #11885 (orange), a real sleepy lizard showing active movement and individual #11533 (blue), a real sleepy lizard showing passive movement, throughout the breeding season. (b) Hourly T_b for a simulated optimising animal (orange) and satisfying animal (blue). (c) Example of daily T_b profile for the same optimising animal during the hottest (orange curve) and coldest (blue curve) day of the breeding season. Dashed horizontal lines show thermal limits of activity period (26–35°C) and black graphics atop (a) represents the sun cycle

extremes when foraging than when retreating to refuges. Our modelling framework directly links these time costs to food availability in the model landscape and to metabolism via satiation, i.e. a gut fullness threshold imposing hunger. Therefore, we can naturally capture how changes in T_b affect gut emptying rates via metabolic rate to drive foraging opportunities and thus movement decisions. By connecting the web of metabolic and heat pathways of the animal (Figure 1; see Figure 2 in Kearney et al., 2010), the IDEBM model shows the feedbacks in time and space between the internal energetics of the animal and external environmental change of the habitat form inescapable, interacting constraints. From these interacting constraints arises complex conditional movement behaviour from simple rules.

We used theory-based estimates of direct movement costs to represent the metabolic investment of movement between different strategies of the sleepy lizard to further interpret differences in minimum (satisficing) and maximum (optimising) movement potential. On average, movement for satisficing animals cost less (Figure 6a), allowing for more metabolic input into structural volume, storage, converted food mass and subsequently reproductive mass (Figure 6b). Despite affording increased space use and more freedom when finding resources, non-essential movement, i.e. socialising, for optimising animals yielded a lower, albeit marginal, metabolic return than satisficing ones after the breeding season across all mass properties. Coupled with the home range overlap of optimising and wild animals (Figure 3), this suggests real sleepy lizards may indeed invest substantial amounts energy into movement with little nutritional return. This is supported by field observations that male sleepy lizards in particular spend large amounts of time mate guarding in addition to foraging (Godfrey, Bradley, Sih, & Bull, 2012; Kerr & Bull, 2006).

Movement is a costly process (Wilson et al., 2013, 2014; Wilson, Husak, Halsey, & Clemente, 2015) and difficult to generalise across models due to the complexity of how metabolic pathways allocate energy and mass to different metabolic functions. This complexity means movement models often apply ad hoc or field-based movement costs (Ayllón et al., 2016; Buchmann, Schurr, Nathan, & Jeltsch, 2011; Kuřakowska et al., 2014; Louzao, Wiegand, Bartumeus, & Weimerskirch, 2014) and thus can overlook or ignore key physical processes essential to energy budget estimates, such as how metabolic rates depend on temperature. We can gain a more structured approach to the problem of integrating movement costs with energy budgets by incorporating these costs into formal metabolic theory. DEB theory applies a metabolic hierarchy to energy allocation via the κ rule (Table 1), where energy diverges to the κ branch to supply somatic maintenance and growth (Equation 2 in Appendix 3 in Supporting information) and the remainder to the $1 - \kappa$ branch for reproduction (Equations 7 and 8 in Appendix 3 in Supporting information). Movement costs could indeed be added to either of these branches, but they are most often considered part of somatic maintenance costs (Kooijman, 2010), as per our simulations. In this case, movement costs compete directly with growth. Because we modelled animals that were near to maximum size, and thus very little energy was being allocated to growth, the costs were mostly manifested as minor reductions in body condition. For juveniles, where a greater

proportion of this energy flow is allocated to growth, the fitness costs of movement would be manifested as reduced growth rate. An alternative would be to impose locomotion costs on the $1 - \kappa$ branch. Here, costs for adults would manifest as reduced size-specific reproductive output, while costs for juveniles would be an increased time to sexual maturity. A mixed strategy is also possible, where a portion of movement costs come from the κ branch and some from the $1 - \kappa$ branch. Indeed, the extra movement costs of male sleepy lizards (Kerr & Bull, 2006) could equate to the energy females allocate to offspring. Exploring these various ways of imposing movement costs, and thus movement decisions in space and time, under the IDEBM framework is an interesting avenue for future research.

Rapidly changing thermal environments from climate change may reduce activity time and consequently increase localised extinction risk (Sinervo et al., 2010). However, animals experience microclimates that vary substantially within and between habitats, on daily cycles (Figure 7), in their spatial patterns (Sears et al., 2011), and in proximity to resources (Kearney, 2013). We found rates of T_b change of simulated satisficing and optimising strategies were similar to observed passive and active movement between the morning (06.00–12.00) and afternoon (12.00–18.00) hours of the day (Figure S2), suggesting that animals incur similar thermoregulatory time costs when exposed to morning and afternoon thermal extremes. For animals to tolerate these costs and exploit available activity time depends on basic individual differences, such as body mass, food requirements, and movement strategy (Huey & Pianka, 1981; Kearney & Porter, 2004; Stevenson, 1985a). For example, small, opportunistic foragers, such as *Sceloporus serrifer*, require more time exposed to thermal extremes to satisfy foraging needs than larger and hardier omnivorous foragers, such as *T. rugosa*. Therefore, a smaller body mass runs a higher risk of overheating and thus restricted dispersal ability (Kearney & Porter, 2004; Sinervo et al., 2010). Indeed, high rates of T_b change on fine scales impose direct physical limits to animals in space due to the trade-offs between choosing to move and the distance required to escape environmental extremes (Sears et al., 2011, 2016); this in turn can restrict movement patterns to localised areas in space, thus limiting available activity time (Grant & Dunham, 1990). Therefore, the challenge for the animal is to balance its movement trade-offs, i.e. the frequency at which they emerge and retreat from and to shelter and use different movement strategies (Figure 4), against available and actual activity time as changing weather shifts activity windows throughout the day and year (Kearney et al., 2009; Stevenson, 1985b; Vickers et al., 2011).

Ideally, a model capturing these detailed individual responses to varying environmental processes ought to be general and applied to biologically relevant scales (Sears & Angilletta, 2015). The IDEBM model achieves these ideals using general principles of energy and mass exchange, realistic microclimatic inputs, and basic movement rules in a spatially explicit context (Figure 1), addressing the need for more detailed physiology-based movement models in space (Sears et al., 2016). This provides a general, bottom-up framework to capture different movement motivations and highlights the importance of attributing individual-based physiological constraints to movement when exploring fine scale patch to home range behaviour (Kearney

& Porter, 2009; Martin, Calenge, Quenette, & Allainé, 2008; Sears & Angilletta, 2015; Sears et al., 2016). Populating the model landscape with realistic fine-scale microclimate inputs generates detailed and varied environmental scenarios. In our simulations, changing resource distribution had no effect on home range size between simulated movement strategies (Figure S1). However, using LIDAR data of the study site to configure resource (food and shade) distribution in space (see insets of Figure S1), the model landscape can simulate realistic changes in habitat structure expected in nature, such as the boom and bust of shady vegetation following rainfall and fire events. This captures movement and behavioural responses to habitat change by allowing users to simulate how environmental disturbances (external cues) influence individual decisions (internal cues).

By combining both internal and external movement drivers, the IDEBM model highlights how food and shade patterns determine suitable movement corridors and the frequency at which activity windows occur and persist based on physiology-driven movement limits. Simulations of home range behaviour from physiology-based estimates shows that the relationship between potential home range patterns and spatial distances among food and refuge sites is subtle, but crucial (Leu, Bashford, Kappeler, & Bull, 2010). We need a solid, bottom-up understanding of this relationship to interpret shade-seeking behaviour in specific habitat contexts (Belliere, Carrascal, & Díaz, 1996; Kearney et al., 2009) or predict home ranges when resources vary in time and space (Figure 3; Tracy & Christian, 1986; Mitchell & Powell, 2004; Moorcroft, Lewis, & Crabtree, 2006; Börger, Dalziel, & Fryxell, 2008). The time animals spend within various activity states (e.g. Searching, Feeding, or Resting) can shift their activity patterns as habitat conditions change. For example, a switch in the frequency of time spent in different states depends on food availability and temperature; after depleting local food sources, animals can increase their searching effort (measured as space use) assuming that suitable conditions, such as more foraging hours in the later and warmer breeding season, permit further foraging (Sears et al., 2016; Sinervo et al., 2010). We show optimising animals searched and foraged more in the later and warmer breeding season (Figure 4a–b). Further, despite a similar gut fullness threshold for foraging, satiating animals in our simulations still only fed less than half as much as optimising animals. Therefore, optimising animals more often transitioned and spent more time overall transitioning among activities, suggesting habitat conditions during this time of year permitted increased searching and foraging (Figure 4a–b), but still induced movement trade-offs by forcing them to regulate their internal state, i.e. shuttling in and out of shade while trying to forage (Figure 4d). Optimising animals, however, displaced further throughout the landscape when feeding, despite spending more time resting and searching than feeding. This implies that, in the short term, the surplus time for optimising animals to move freely during available activity hours meant locating food patches or at least settling in areas where food was more abundant, such as shade adjacent to lots of food, was easier (Figure 5). In the long term, however, this benefit yielded little energetic return (Figure 6b). These results also suggest that directional (gravitating towards food) over correlated random movement is more

useful for negotiating landscapes when animals are constrained by physiological limits to movement (Fronhofer, Hovestadt, & Poethke, 2013), such as thermal limits and movement costs, including turn costs (Wilson et al., 2013). Building movement models around different behavioural states fills necessary biological gaps in model development and addresses inherent model fitting issues across varying time scales (Morales, Haydon, Frair, Holsinger, & Fryxell, 2004). The IDEBM model adds to these important modelling criteria by incorporating a theoretical basis to the mechanisms driving movement, thereby providing a generic framework to address movement costs and motivations across scales.

11 | LIMITATIONS AND FUTURE WORK

Feedback delays between the rate at which activity states update and the scale of the decision-making model time steps could influence overall activity budgets and thus space use over time for each activity state. This is a potential artefact of the model update procedures that requires further fine tuning. The similar home range sizes of animals under sparse and dense resource distributions was surprising (Figure S1). Future work could consider simulating habitats with larger thermal extremes (Blouin-Demers & Nadeau, 2005; Christian & Weavers, 1996), different topography (Sears et al., 2011) and ecoclines (Sunday et al., 2014), or similar resource distributions, but under increased warming scenarios. Our aim here is to deconstruct how the subtlety of habitat arrangement influences displacement and home range behaviour.

Because the model assumes 50% shade levels and no burrowing, some simulated animals reached unnaturally high T_b on the hottest day of the season (Figure 7c). Future model configurations incorporating varying shade levels and perhaps burrowing behaviour would refine T_b outputs during resting and shade-seeking behaviour. Further work dissecting how the consequences of direct movement costs, including turn costs (Wilson et al., 2013), change throughout the animal lifecycle is also needed. Our study species is long-lived and slow to mature. By simulating longer time periods, the life-history consequences of movement costs will become more apparent for this species, including how energy allocated among maintenance, growth, and movement shapes juvenile dispersal periods and gender differences in movement for females encumbered by the heavy metabolic demands of reproductive egg investment. We can also use the interacting internal and external drivers of the model to summarise basal metabolic rates of endotherms and thus use a similar approach to how internal energy and water costs constrain their movement decisions (Kearney & Porter, 2009; Porter, Munger, Stewart, Budaraju, & Jaeger, 1994). Finally, the physiology-driven mechanics of the model opens opportunities to explore within-species behaviour differences, including territoriality and interacting individuals (Leu, Farine, Wey, Sih, & Bull, 2016; Spiegel, Leu, Bull, & Sih, 2017; Spiegel et al., 2016), as well as scaling to population-level responses, such as using GPS data of movement rates to forecast range expansion of invasive species fronts,

e.g. cane toad dispersal (Phillips, Brown, Greenlees, Webb, & Shine, 2007).

12 | CONCLUSIONS

Here, we presented an individual-based movement model built on general biophysical and metabolic principles of the individual animal and its direct relationship with food and weather in space and time. By explicitly capturing the physical limits driving movement, the IDEBM model presents a realistic and flexible approach for predicting current and future movement and home range activity under changing food and weather. This flexibility also makes the model robust to different time and space scales, so animals can experience different weather and habitats throughout the year. That is, we can refine how we interpret behavioural limits necessary for survival across scales and the physiological and ecological limits under which animals persist over their lifetime. The theory-driven estimates of movement costs in the model represents a reliable physiological understanding of movement and bottom-up forecasting of fine scale environmental change on habitat use and interpreting the ecological niche. Using a general, first principles approach to animal movement, the IDEBM model is thus suitable for tackling a wide range of questions in ecology and behaviour to improve our understanding of how spatial patterns of resources and microclimates influence complex behaviour, especially in the context of environmental change.

ACKNOWLEDGEMENTS

We thank Mark Burgman, Michael Bode, Stephan Leu, Roger Nisbet and Mike Sears for helpful insight and constructive discussion on our ideas and Daniel Ayllón, Pascal Fust, Eduardo Arraut, Hugo Thierry and Ben Martin for insight and input on early model development. We also thank two anonymous reviewers and Luca Börger for their helpful comments and feedback that greatly improved this manuscript. This research was funded by an Australian Postgraduate Award and Holsworth Research Grant to M.M. and ARC Discovery grants DP140101240 and DP110102813 to M.R.K. and DP0877384 to C.M.B. It was also supported by a resource allocation grant from the Victorian Life Sciences Computation Initiative to M.R.K. and The Centre of Excellence for Biosecurity Risk Analysis. The work was conducted under Flinders Animal Welfare Permit E232 and South Australian Department of Environment Water and Natural Resources Research Permit A23436. We dedicate this work to the memory of Prof. Mike Bull who passed away before the work was completed.

AUTHORS' CONTRIBUTIONS

M.M. conceived and wrote the manuscript, developed the simulation models and parameterised the energy budget model, C.M.B. collected field data and contributed to manuscript revisions and M.R.K. wrote the manuscript and developed the microclimate model, the "NICHEMAPR" R package, and parameterised the energy budget model. All authors contributed to revisions and approved of the final versions.

DATA ACCESSIBILITY

Full code for the microclimate model ("onelump_varenv.R"), energy budget model ("DEB.R"), NetLogo code for the individual-based decision-making model (Appendix 1 in Supporting information), R code for the simulation model (Appendix 2 in Supporting information), and microclimate data for sun ("metout.csv" and "soil.csv") and shade ("shadmet.csv" and "shadsoil.csv") conditions for the model landscape are available in the Supplementary material. All Supplementary Material is also available at <https://doi.org/10.5281/zenodo.998145>.

ORCID

Matthew Malishev  <http://orcid.org/0000-0002-8507-4433>

Michael R. Kearney  <http://orcid.org/0000-0002-3349-8744>

REFERENCES

- Adolph, S. C., & Porter, W. P. (1993). Temperature, activity and lizard life histories. *American Naturalist*, *142*, 273–295.
- Auburn, Z. M., Bull, C. M., & Kerr, G. D. (2009). The visual perceptual range of a lizard, *Tiliqua rugosa*. *Journal of Ethology*, *27*, 75–81.
- Ayllón, D., Railsback, S. F., Vincenzi, S., Groeneveld, J., Almodóvar, A., & Grimm, V. (2016). InSTREAM-Gen: Modelling eco-evolutionary dynamics of trout populations under anthropogenic environmental change. *Ecological Modelling*, *326*, 36–53.
- Bateman, A. W., Lewis, M. A., Gall, G., Manser, M. B., & Clutton-Brock, T. H. (2015). Territoriality and home-range dynamics in meerkats, *Suricata suricatta*: A mechanistic modelling approach. *The Journal of Animal Ecology*, *84*, 260–271.
- Belliure, J., Carrascal, L. M., & Díaz, J. A. (1996). Covariation of thermal biology and foraging mode in two mediterranean lacertid lizards. *Ecology*, *77*, 1163–1173.
- Blouin-Demers, G., & Nadeau, P. (2005). The cost-benefit model of thermoregulation does not predict lizard thermoregulatory behavior. *Ecology*, *86*, 560–566.
- Börger, L., Dalziel, B. D., & Fryxell, J. M. (2008). Are there general mechanisms of animal home range behaviour? A review and prospects for future research. *Ecology Letters*, *11*, 637–650.
- Brown, J. H., Gillooly, J. F., Allen, A. P., Savage, V. M., & West, G. B. (2004). Toward a metabolic theory of ecology. *Ecology*, *85*, 1771–1789.
- Buchmann, C. M., Schurr, F. M., Nathan, R., & Jeltsch, F. (2011). An allometric model of home range formation explains the structuring of animal communities exploiting heterogeneous resources. *Oikos*, *120*, 106–118.
- Buckley, L. B. (2008). Linking traits to energetics and population dynamics to predict lizard ranges in changing environments. *The American Naturalist*, *171*, 1–19.
- Chambers, J. M., Becker, R. A., & Wilks, A. R. (1988). *The new S language: A programming environment for data analysis and graphics*. Monterey, CA: Wadsworth and Brooks.
- Christian, K., Tracey, C. R., & Porter, W. P. (1983). Seasonal shifts in body temperature and use of microhabitats by Galapagos land iguanas (*Conolophus pallidus*). *Ecology*, *64*, 463–468.
- Christian, K. A., & Weavers, B. W. (1996). Thermoregulation of monitor lizards in Australia: An evaluation of methods in thermal biology. *Ecological Monographs*, *66*, 139–157.
- Clissold, F. J., Coggan, N., & Simpson, S. J. (2013). Insect herbivores can choose microclimates to achieve nutritional homeostasis. *The Journal of Experimental Biology*, *216*(Pt 11), 2089–2096.

- Clobert, J., Le Galliard, J.-F., Cote, J., Meylan, S., & Massot, M. (2009). Informed dispersal, heterogeneity in animal dispersal syndromes and the dynamics of spatially structured populations. *Ecology Letters*, *12*, 197–209.
- Crozier, L., & Dwyer, G. (2006). Combining population-dynamic and eco-physiological models to predict climate-induced insect range shifts. *The American Naturalist*, *167*, 853–866.
- Davies, Z. G., Wilson, R. J., Coles, S., & Thomas, C. D. (2006). Changing habitat associations of a thermally constrained species, the silver-spotted skipper butterfly, in response to climate warming. *Journal of Animal Ecology*, *75*, 247–256.
- Fahrig, L. (2007). Non-optimal animal movement in human-altered landscapes. *Functional Ecology*, *21*, 1003–1015.
- Franklin, C. E., Davison, W., & Seebacher, F. (2007). Antarctic fish can compensate for rising temperatures: Thermal acclimation of cardiac performance in *Pagothenia borchgrevinki*. *The Journal of Experimental Biology*, *210*(Pt 17), 3068–3074.
- Fronhofer, E. A., Hovestadt, T., & Poethke, H. J. (2013). From random walks to informed movement. *Oikos*, *122*, 857–866.
- Gates, D. M. (1980). *Biophysical ecology*. New York, NY: Springer Verlag.
- Godfrey, S. S., Bradley, J. K., Sih, A., & Bull, C. M. (2012). Lovers and fighters in sleepy lizard land: Where do aggressive males fit in a social network? *Animal Behaviour*, *83*, 209–215.
- Grant, B. W., & Dunham, A. E. (1990). Elevational covariation in environmental constraints and life histories of the desert lizard *Sceloporus merriami*. *Ecology*, *71*, 1765–1776.
- Grimm, V., Berger, U., Bastiansen, F., Eliassen, S., Ginot, V., Giske, J., ... DeAngelis, D. L. (2006). A standard protocol for describing individual-based and agent-based models. *Ecological Modelling*, *198*, 115–126.
- Helmuth, B. S. T., & Hofmann, G. E. (2001). Microhabitats, thermal heterogeneity, and patterns of physiological stress in the rocky intertidal zone. *Biological Bulletin*, *201*, 374–384.
- Helmuth, B., Kingsolver, J. G., & Carrington, E. (2005). Biophysics, physiological ecology, and climate change: Does mechanism matter? *Annual Review of Physiology*, *67*, 177–201.
- Holling, C. S. (1959). Some characteristics of simple types of predation and parasitism. *The Canadian Entomologist*, *91*, 385–398.
- Huey, R. B. (1991). Physiological consequences of habitat selection. *The American Naturalist*, *137*, 91–115.
- Huey, R. B., & Pianka, E. R. (1981). Ecological consequences of foraging mode. *Ecology*, *62*, 991–999.
- John-Alder, H. B., Garland, T., & Bennett, A. F. (1986). Locomotory capacities, oxygen consumption, and the cost of locomotion of the shingle-back lizard (*Trachydosaurus rugosus*). *Physiological Zoology*, *59*, 523–531.
- Jones, D. A., Wang, W., & Fawcett, R. (2009). High-quality spatial climate data-sets for Australia. *Australian Meteorological and Oceanographic Journal*, *58*, 233–248.
- Kays, R., Crofoot, M. C., Jetz, W., & Wikelski, M. (2015). Terrestrial animal tracking as an eye on life and planet. *Science*, *348*, aaa2478.
- Kearney, M. (2012). Metabolic theory, life history and the distribution of a terrestrial ectotherm. *Functional Ecology*, *26*, 167–179.
- Kearney, M. R. (2013). Activity restriction and the mechanistic basis for extinctions under climate warming. *Ecology Letters*, *16*, 1470–1479.
- Kearney, M. R., & Porter, W. P. (2004). Mapping the fundamental niche: Physiology, climate, and the distribution of a nocturnal lizard. *Ecology*, *85*, 3119–3131.
- Kearney, M. R., & Porter, W. P. (2009). Mechanistic niche modelling: Combining physiological and spatial data to predict species' ranges. *Ecology Letters*, *12*, 334–350.
- Kearney, M. R., Shine, R., & Porter, W. P. (2009). The potential for behavioural thermoregulation to buffer “cold-blooded” animals against climate warming. *Proceedings of the National Academy of Sciences of the USA*, *106*, 3835–3840.
- Kearney, M. R., Simpson, S. J., Raubenheimer, D., & Helmuth, B. (2010). Modelling the ecological niche from functional traits. *Philosophical Transactions of the Royal Society B-Biological Sciences*, *365*, 3469–3483.
- Kearney, M. R., Simpson, S. J., Raubenheimer, D., & Kooijman, S. A. L. M. (2013). Balancing heat, water and nutrients under environmental change: A thermodynamic niche framework. *Functional Ecology*, *27*, 950–966.
- Kerr, G. D., & Bull, C. M. (2006). Movement patterns in the monogamous sleepy lizard (*Tiliqua rugosa*): effects of gender, drought, time of year and time of day. *Journal of Zoology*, *269*, 137–147.
- Kerr, G. D., Bull, C. M., & Cottrell, G. R. (2004). Use of an “on board” datalogger to determine lizard activity patterns, body temperature and microhabitat use for extended periods in the field. *Wildlife Research*, *31*, 171–176.
- Kooijman, S. A. L. M. (2010). *Dynamic energy budget theory*. Cambridge, UK: Cambridge University Press.
- Kuřakowska, K., Kuřakowski, T. M., Inglis, I. R., Smith, G. C., Haynes, P. J., Prosser, P., ... Sibly, R. M. (2014). Using an individual-based model to select among alternative foraging strategies of woodpeckers: Data support a memory-based model with a flocking mechanism. *Ecological Modelling*, *280*, 89–101.
- Leu, S. T., Bashford, J., Kappeler, P. M., & Bull, C. M. (2010). Association networks reveal social organization in the sleepy lizard. *Animal Behaviour*, *79*, 217–225.
- Leu, S. T., Farine, D. R., Wey, T. W., Sih, A., & Bull, C. M. (2016). Environment modulates population social structure: Experimental evidence from replicated social networks of wild lizards. *Animal Behaviour*, *111*, 23–31.
- Lika, K., Kearney, M. R., Freitas, V., van der Veer, H. W., van der Meer, J., Wijsman, J. W. M., ... Kooijman, S. A. L. M. (2011). The “covariation method” for estimating the parameters of the standard Dynamic Energy Budget model I: Philosophy and approach. *Journal of Sea Research*, *66*, 270–277.
- Louzao, M., Wiegand, T., Bartumeus, F., & Weimerskirch, H. (2014). Coupling instantaneous energy-budget models and behavioural mode analysis to estimate optimal foraging strategy: An example with wandering albatrosses. *Movement Ecology*, *2*, 8.
- Martin, J., Calenge, C., Quenette, P. Y., & Allainé, D. (2008). Importance of movement constraints in habitat selection studies. *Ecological Modelling*, *213*, 257–262.
- McClure, M., Cannell, E., & Despland, E. (2011). Thermal ecology and behaviour of the nomadic social forager *Malacosoma disstria*. *Physiological Entomology*, *36*, 120–127.
- McVicar, T. R., Van Niel, T. G., Li, L. T., Roderick, M. L., Rayner, D. P., Ricciardulli, L., & Donohue, R. J. (2008). Wind speed climatology and trends for Australia, 1975–2006: Capturing the stilling phenomenon and comparison with near-surface reanalysis output. *Geophysical Research Letters*, *35*, L20403.
- Mitchell, M. S., & Powell, R. A. (2004). A mechanistic home range model for optimal use of spatially distributed resources. *Ecological Modelling*, *177*, 209–232.
- Mitchell, M. S., & Powell, R. A. (2012). Foraging optimally for home ranges. *Journal of Mammalogy*, *93*, 917–928.
- Moorcroft, P. R., Lewis, M. A., & Crabtree, R. L. (2006). Mechanistic home range models capture spatial patterns and dynamics of coyote territories in Yellowstone. *Proceedings of the Royal Society of London B: Biological Sciences*, *273*, 1651–1659.
- Morales, J. M., Haydon, D. T., Frair, J., Holsinger, K. E., & Fryxell, J. M. (2004). Extracting more out of relocation data: Building movement models as mixtures of random walks. *Ecology*, *85*, 2436–2445.
- Müller, T., Fagan, W. F., & Grimm, V. (2011). Integrating individual search and navigation behaviors in mechanistic movement models. *Theoretical Ecology*, *4*, 341–355.
- Nisbet, R. M., Muller, E. B., Lika, K., & Kooijman, S. A. L. M. (2000). From molecules to ecosystems through dynamic energy budget models. *Journal of Animal Ecology*, *69*, 913–926.
- Pamula, Y. (1997). *Ecological and physiological aspects of reproduction in the viviparous skink Tiliqua rugosa*. South Australia, Australia: Flinders University.

- Pearson, R. G., Thuiller, W., Araújo, M. B., Martinez-Meyer, E., Brotons, L., McClean, C., ... Lees, D. C. (2006). Model-based uncertainty in species range prediction. *Journal of Biogeography*, 33, 1704–1711.
- Phillips, B. L., Brown, G. P., Greenlees, M., Webb, J. K., & Shine, R. (2007). Rapid expansion of the cane toad (*Bufo marinus*) invasion front in tropical Australia. *Austral Ecology*, 32, 169–176.
- Porter, W. P., Mitchell, J. W., Beckman, W. A., & DeWitt, C. B. (1973). Behavioral implications of mechanistic ecology. *Oecologia*, 13, 1–54.
- Porter, W. P., Munger, J. C., Stewart, W. E., Budaraju, S., & Jaeger, J. (1994). Endotherm energetics - from a scalable individual-based model to ecological applications. *Australian Journal of Zoology*, 42, 125–162.
- Porter, W. P., Vakharia, N., Klousie, W. D., & Duffy, D. (2006). Po'ouli landscape bioinformatics models predict energetics, behavior, diets, and distribution on Maui. *Integrative and Comparative Biology*, 46, 1143–1158.
- R Development Core Team. (2015). *R: A language and environment for statistical computing*. Vienna, Austria: R Foundation for Statistical Computing. Available at: <http://www.R-project.org/>.
- Railsback, S. F., Lamberson, R. H., Harvey, B. C., & Duffy, W. E. (1999). Movement rules for individual-based models of stream fish. *Ecological Modelling*, 123, 73–89.
- Randin, C. F., Dirnböck, T., Dullinger, S., Zimmermann, N. E., Zappa, M., & Guisan, A. (2006). Are niche-based species distribution models transferable in space? *Journal of Biogeography*, 33, 1689–1703.
- Schick, R. S., Loarie, S. R., Colchero, F., Best, B. D., Boustany, A., Conde, D. A., ... Clark, J. S. (2008). Understanding movement data and movement processes: Current and emerging directions. *Ecology Letters*, 11, 1338–1350.
- Schurr, F. M., Pagel, J., Cabral, J. S., Groeneveld, J., Bykova, O., O'Hara, R. B., ... Zimmermann, N. E. (2012). How to understand species' niches and range dynamics: A demographic research agenda for biogeography. *Journal of Biogeography*, 39, 2146–2162.
- Sears, M. W., & Angilletta, M. J. (2015). Costs and benefits of thermoregulation revisited: Both the heterogeneity and spatial structure of temperature drive energetic costs. *American Naturalist*, 185, E94–E102.
- Sears, M. W., Raskin, E., & Angilletta, M. J. (2011). The world is not flat: Defining relevant thermal landscapes in the context of climate change. *Integrative and Comparative Biology*, 51, 666–675.
- Sears, M. W., Angilletta Jr., M. J., Schuler, M. S., Borchert, J., Dilliplane, K. F., Stegman, M., ... Mitchell, W. A. (2016). Configuration of the thermal landscape determines thermoregulatory performance of ectotherms. *Proceedings of the National Academy of Sciences of the USA*, 113, 10595–10600.
- Shaw, A. K., & Couzin, I. D. (2013). Migration or residency? The evolution of movement behavior and information usage in seasonal environments. *The American Naturalist*, 181, 114–124.
- Shelly, T. E. (1982). Comparative foraging behavior of light- versus shade-seeking adult damselflies in a lowland Neotropical forest (Odonata: Zygoptera). *Physiological Zoology*, 55, 335–343.
- Sinervo, B., de Mendez-de-la-Cruz, F., Miles, D. B., Heulin, B., Bastiaans, E., Villagran-Santa Cruz, M., ... Sites, J. W. (2010). Erosion of lizard diversity by climate change and altered thermal niches. *Science*, 328, 894–899.
- Snider, A. T., & Bowler, J. K. (1992). *Longevity of reptiles and amphibians in North American collections*, Herpetological Circular no. 21. Milwaukee, WI: SSAR Publications.
- Spiegel, O., Leu, S. T., Bull, C. M., & Sih, A. (2017). What's your move? Movement as a link between personality and spatial dynamics in animal populations. *Ecology Letters*, 20, 3–18.
- Spiegel, O., Leu, S. T., Sih, A., & Bull, C. M. (2016). Socially interacting or indifferent neighbours? Randomization of movement paths to tease apart social preference and spatial constraints. *Methods in Ecology and Evolution*, 7, 971–979.
- Stamps, J. A. (2007). Growth-mortality tradeoffs and “personality traits” in animals. *Ecology Letters*, 10, 355–363.
- Stevenson, R. D. (1985a). Body size and limits to the daily range of body temperature in terrestrial ectotherms. *The American Naturalist*, 125, 102–117.
- Stevenson, R. D. (1985b). The relative importance of behavioral and physiological adjustments controlling body temperature in terrestrial ectotherms. *American Naturalist*, 126, 362–386.
- Sunday, J. M., Bates, A. E., Kearney, M. R., Colwell, R. K., Dulvy, N. K., Longino, J. T., & Huey, R. B. (2014). Thermal-safety margins and the necessity of thermoregulatory behavior across latitude and elevation. *Proceedings of the National Academy of Sciences*, 111, 5610–5615.
- Thiele, J. C., Kurth, W., & Grimm, V. (2012). RNetLogo: An R package for running and exploring individual-based models implemented in NetLogo. *Methods in Ecology and Evolution*, 3, 480–483.
- Tracy, C. R., & Christian, K. A. (1986). Ecological relations among space, time and thermal niche axes. *Ecology*, 67, 609–615.
- Vickers, M., Manicom, C., & Schwarzkopf, L. (2011). Extending the cost-benefit model of thermoregulation: High-temperature environments. *American Naturalist*, 177, 452–461.
- Villén-Pérez, S., Carrascal, L. M., & Seoane, J. (2013). Foraging patch selection in winter: A balance between predation risk and thermoregulation benefit. *PLoS ONE*, 8, e68448.
- Wang, M., & Grimm, V. (2007). Home range dynamics and population regulation: An individual-based model of the common shrew *Sorex araneus*. *Ecological Modelling*, 205, 397–409.
- Werner, E. E., & Anholt, B. R. (1993). Ecological consequences of the trade-off between growth and mortality rates mediated by foraging activity. *The American Naturalist*, 142, 242–272.
- Wilensky, U. (1999). *NetLogo. Center for connected learning and computer based modeling*. Evanston, IL: Northwestern University. Retrieved from <http://ccl.northwestern.edu/netlogo/>.
- Wilson, K. J., & Lee, A. K. (1974). Energy expenditure of Large Herbivorous Lizard. *Copeia*, 2, 338–348.
- Wilson, R. P., Griffiths, I. W., Legg, P. A., Friswell, M. I., Bidder, O. R., Halsey, L. G., ... Shepard, E. L. C. (2013). Turn costs change the value of animal search paths. *Ecology Letters*, 16, 1145–1150.
- Wilson, R. P., Grundy, E., Massy, R., Soltis, J., Tysse, B., Holton, M., ... Butt, T. (2014). Wild state secrets: Ultra-sensitive measurement of micro-movement can reveal internal processes in animals. *Frontiers in Ecology and the Environment*, 12, 582–587.
- Wilson, R. S., Husak, J. F., Halsey, L. G., & Clemente, C. J. (2015). Predicting the movement speeds of animals in natural environments. *Integrative and Comparative Biology*, 55, 1125–1141.

SUPPORTING INFORMATION

Additional Supporting Information may be found online in the supporting information tab for this article.

How to cite this article: Malishev M, Michael Bull C, Kearney MR. An individual-based model of ectotherm movement integrating metabolic and microclimatic constraints. *Methods Ecol Evol*. 2018;9:472–489. <https://doi.org/10.1111/2041-210X.12909>